



Cite this article: Namadurai S, Yereddi NR, Cusdin FS, Huang CL-H, Chirgadze DY, Jackson AP. 2015 A new look at sodium channel β subunits. *Open Biol.* 5: 140192. <http://dx.doi.org/10.1098/rsob.140192>

Received: 15 October 2014

Accepted: 6 December 2014

Subject Area:

biochemistry/molecular biology/neuroscience

Keywords:

sodium channel β subunits, X-ray crystallography, ion channelopathies

Author for correspondence:

Antony P. Jackson

e-mail: apj10@cam.ac.uk

[†]Present address: Medimmune, Granta Park, Cambridge CB21 6GH, UK.

A new look at sodium channel β subunits

Sivakumar Namadurai¹, Nikitha R. Yereddi¹, Fiona S. Cusdin^{1,†},

Christopher L.-H. Huang², Dimitri Y. Chirgadze¹ and Antony P. Jackson¹

¹Department of Biochemistry, University of Cambridge, Tennis Court Road, Cambridge CB2 1QW, UK

²Physiological Laboratory, University of Cambridge, Cambridge CB2 3EG, UK

APJ, 0000-0002-2895-7387

1. Summary

Voltage-gated sodium (Na_v) channels are intrinsic plasma membrane proteins that initiate the action potential in electrically excitable cells. They are a major focus of research in neurobiology, structural biology, membrane biology and pharmacology. Mutations in Na_v channels are implicated in a wide variety of inherited pathologies, including cardiac conduction diseases, myotonic conditions, epilepsy and chronic pain syndromes. Drugs active against Na_v channels are used as local anaesthetics, anti-arrhythmics, analgesics and anti-convulsants. The Na_v channels are composed of a pore-forming α subunit and associated β subunits. The β subunits are members of the immunoglobulin (Ig) domain family of cell-adhesion molecules. They modulate multiple aspects of Na_v channel behaviour and play critical roles in controlling neuronal excitability. The recently published atomic resolution structures of the human $\beta 3$ and $\beta 4$ subunit Ig domains open a new chapter in the study of these molecules. In particular, the discovery that $\beta 3$ subunits form trimers suggests that Na_v channel oligomerization may contribute to the functional properties of some β subunits.

2. Introduction

Electrically excitable cells such as neurons and myocytes communicate via action potentials, and voltage-gated sodium (Na_v) channels play an essential role in this process (figure 1). The vertebrate Na_v channel α subunit is a single polypeptide chain (molecular mass approx. 260 kDa) that contains the ion-selective component. There are 10 mammalian α subunit genes encoding the proteins $\text{Na}_v 1.1$ – $\text{Na}_v 1.9$, and an atypical channel, Na_x . Separate α subunit isoforms are expressed in tissue-specific patterns and exhibit differences in gating behaviour that tailor them for distinct physiological roles [1]. Each vertebrate Na_v α subunit contains four homologous but non-identical domains (I–IV), each of which contains six transmembrane helical segments (S1–S6) (figure 2*a*). The domains assemble around the central ion-selective pore [2]. Evidence based on μ conotoxin GIIIA binding suggests that the domains may be organized in a clockwise orientation as viewed from above the extracellular surface [3].

Currently, there are no high-resolution atomic structures of the complete vertebrate Na_v channel α subunit. However, the crystal structures of bacterial Na_v channels in different conformational states [4–6] (figure 2*b*) and a chimeric voltage-gated potassium (K_v) channel [7] have been solved. They have provided rich insights into the molecular basis of channel gating. All of the channels with solved structures are homotetramers rather than a single molecule, so they lack the sequence specializations found in the vertebrate Na_v channel α subunit, such as the distinct extracellular regions, the intracellular linkers between domains and the unique carboxy-terminus (figure 2*a*). Nevertheless, the basic domain organization of the vertebrate Na_v channel is likely to be similar to the subunit organization of the bacterial Na_v channels and the K_v channel [8]. Using these high-resolution structures as guides, we can say that helices S5 and S6 and the

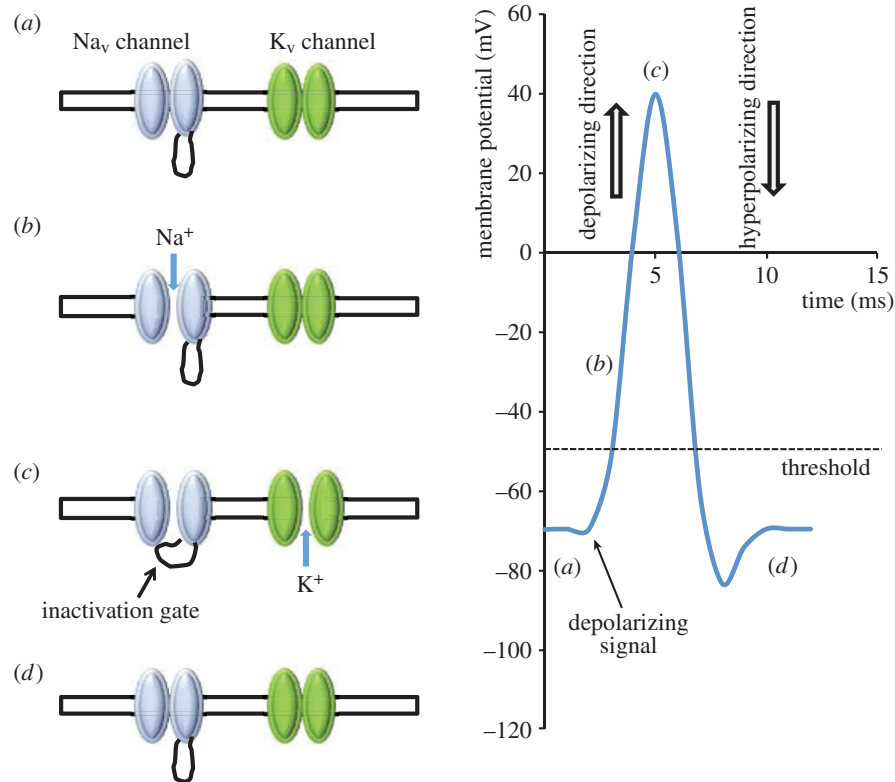


Figure 1. A simplified cartoon showing the main events underlying the action potential. (a) Neurons and other electrically excitable cells maintain a plasma membrane resting potential of about -70 mV (the membrane potential is defined relative to the extracellular medium; a potential of -70 mV implies that the cell interior is negative relative to the exterior). The negative resting membrane potential is largely set by the greater membrane permeability of potassium ions compared with that of sodium ions. This occurs in the presence of a high intracellular potassium ion concentration relative to the extracellular media, and a high extracellular to intracellular sodium ion concentration generated by sodium potassium ATPase activity. Under resting conditions, both voltage-gated sodium (Na_v) and voltage-gated potassium (K_v) channels are closed. The Na_v channels begin to open in response to local membrane depolarization (generated for example by the action of an ionotropic neurotransmitter on its receptor). (b) The net inward flow of sodium ions causes further depolarization that opens more Na_v channels, which in turn causes even greater sodium ion entry and further depolarization. This positive feedback ensures the action potential generates a rapid 'all or nothing' response, whenever the initial stimulus is above a threshold value (here set at -50 mV). (c) In the 'fast inactivation pathway', sodium channels enter an inactive state after a few milliseconds, whereby they cannot respond to any further membrane depolarization signals. Fast inactivation is driven by a conformational change in which a hydrophobic sequence (the 'inactivation gate') lying within the cytoplasmic loop between domains III and IV moves to block the inner mouth of the pore (see text). As a result, the action potential can only be propagated in the forward direction. The subsequent opening of voltage-gated potassium (K_v) channels allows potassium ions to move out of the cell, down their electrochemical gradient. (d) This moves the membrane potential in the hyperpolarizing direction, restores the membrane to its resting potential and enables the Na_v channels to recover from inactivation by returning to their closed conformation.

pore loop regions that connect them form the ion-selective pore module. Helices S1–S4 of each domain comprise the voltage sensor and lie on the outer rim of the pore module, at each corner of the α subunit (figure 2*b*). Helix S4 of each voltage sensor is amphipathic, with one face positively charged (figure 2*a,b*). In response to the electric field changes produced by membrane depolarization, helix S4 moves towards the extracellular face of the membrane, thereby initiating conformational changes that open the pore [4,7]. The voltage sensors of domains I–III show the fastest kinetics and allow ion flow to begin [9]. The domain IV voltage sensor responds more slowly. Its movement frees an intracellular linker called the inactivation gate that connects helix S6 of domain III with helix S1 of domain IV (figure 2*a*) [10,11]. As a result, the inactivation gate can now move to occlude the pore and drive the channel into an inactivated state (figure 1). Thus, Na_v channel activation and inactivation are structurally, mechanistically and functionally linked [8,12].

Most Na_v channels isolated from vertebrate cells contain associated β subunits. There are four β subunit genes (*Scn1b–Scn4b*) encoding proteins $\beta 1–\beta 4$, respectively [13,14]. Alternative splicing of the *Scn1b* gene adds further

diversity to the $\beta 1$ protein [15]. As with the α subunits, individual β subunits are expressed with distinct tissue specificities [16]. All β subunits are type 1 intrinsic membrane proteins. The extracellular amino-terminal region contains a single V-type immunoglobulin (Ig) domain and a short 'neck'. This is connected to a single α -helical transmembrane domain and a carboxy-terminal intracellular region (figure 2*a*). However, the primary sequences of the $\beta 1$ and $\beta 3$ subunits are more closely related to each other than either is to $\beta 2$ or $\beta 4$ [17]. The $\beta 1$ and $\beta 3$ subunits are non-covalently bound to the α subunit, but the $\beta 2$ and $\beta 4$ subunits are covalently attached to the α subunit via an inter-subunit disulfide bond [18,19].

The β subunits can increase peak current density by increasing the amount of channels in the plasma membrane [13]. They also shift the voltage range over which activation and inactivation occur, and they enhance the rates of inactivation and recovery from inactivation [20,21]. They therefore influence many of the key conformational changes that Na_v channels undergo during the action potential cycle [13,16]. Although their gating effects can be subtle, they are clearly important. Mice lacking individual β subunits show

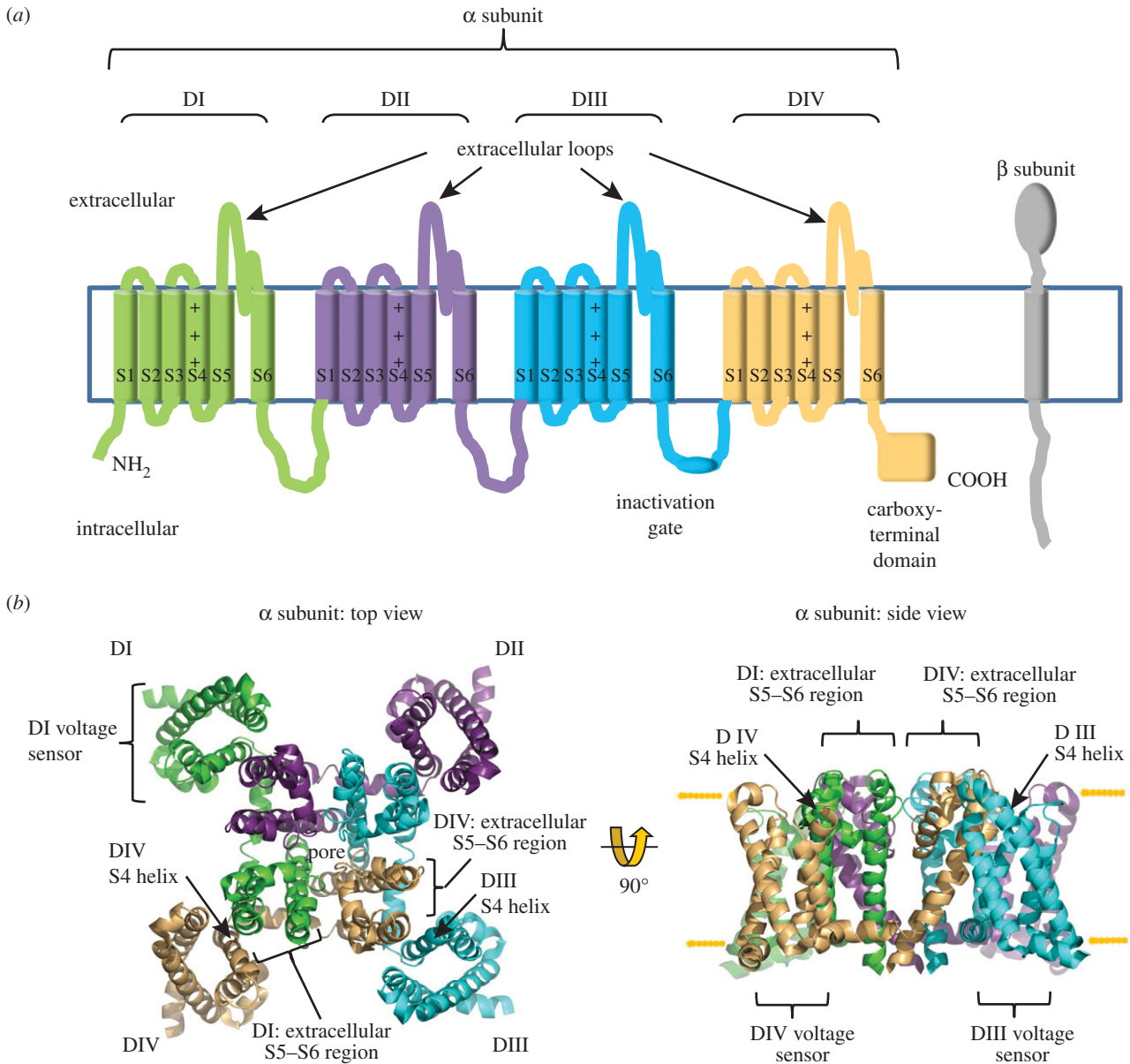


Figure 2. The subunit organization of the voltage-gated Na_v channel. (a) Cartoon topology of the α and β subunits. Within the α subunit, domains I–IV, the amphipathic helix S4 of the voltage sensors, the extracellular region between helices S5 and S6, the fast inactivation gate and the carboxy-terminus are shown. (b) Top view from the extracellular face and side view of the Na_v channel from the bacterium *Arcobacter butzeri* (PDB ID code 3RVY). Using this structure as a guide, the inferred position of each vertebrate α subunit domain (I–IV) is shown colour-coded to match figure 2a. The location of the voltage sensors with the S4 helix for domains III and IV, and the likely position of the S5–S6 extracellular regions of domains I and IV, are indicated.

a range of isoform-specific pathologies such as epilepsy, ataxia and cardiac conduction diseases. Mutations in the β subunits are associated with a number of human inherited diseases, including epilepsy, neuropathies, cardiac conduction diseases and some types of cancer [13,22].

Site-directed mutagenesis has been used to study the function of β subunits. But these experiments were interpreted using structures inferred from homology modelling [23–25], which is inevitably indirect. However, the structures of the human β_3 and β_4 subunit Ig domains have recently been solved at atomic resolution by X-ray crystallography [26,27], and should now allow for much clearer functional insights. In this review, we will focus on the new structural determinations, and consider their pathophysiological implications. For a more in-depth discussion of additional aspects of β subunit biology, especially the roles of these molecules in development, signal transduction and their potential as

pharmacological targets, we recommend other recent reviews [13,16,22,28].

3. The structure of the Na_v channel β_3 subunit Ig domain and implications for the β_1 structure

The X-ray structure of the human β_3 Ig domain has been solved to a resolution of 2.5 Å. Surprisingly, it forms a trimer in the asymmetric unit (figure 3a). This is not a crystal packing artefact: super-resolution imaging detected trimeric full-length β_3 subunits as a major species in the plasma membrane of HEK293 cells [27]. Moreover, atomic force microscopy (AFM) imaged full-length β_3 subunit monomers, dimers and trimers isolated from transfected cells. The trimer is consistent

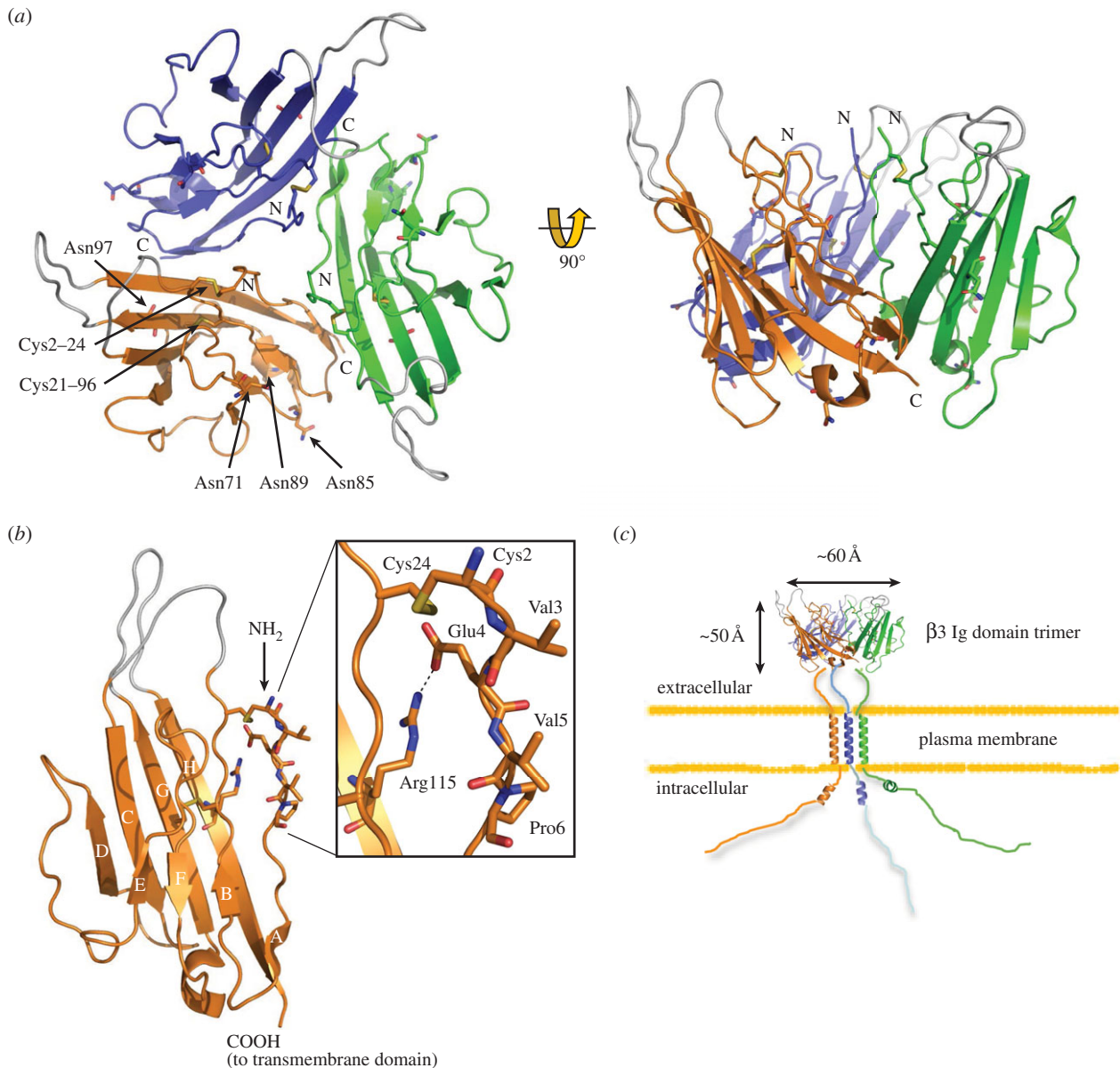


Figure 3. The atomic resolution structure of the $\beta 3$ subunit Ig domain (PDB ID code 4L1D). (a) Diagram showing the arrangement of the $\beta 3$ trimer. Amino (N) and carboxyl (C) termini are labelled. The Cys21–96 disulfide bond and the Cys2–24 disulfide bonds are labelled on the orange protomer. Potential N-linked glycosylation sites Asn71, Asn85, Asn89 and Asn97 are shown as sticks and labelled for the orange protomer. Loops that are not resolved in the electron density maps due to local disorder are shown in grey at their most probable plausible positions. (b) Close-up of the single Na, $\beta 3$ subunit Ig domain protomer. Residues correspond to loops not visible in the electron density maps due to local disorder are shown in grey. A close-up of the region surrounding the trimer interface is shown in the box. (c) Cartoon of the full-length $\beta 3$ trimer as it may appear on the plasma membrane, with correct dimensions. Note: in these diagrams, the amino acids are numbered from the first residue of the mature protein (i.e. lacking the endoplasmic reticulum targeting signal) [27].

with previous evidence showing that when expressed in cells, the full-length $\beta 3$ subunits self-associate in *cis*, and that the Ig domain is necessary for this interaction [25].

The Ig domain is one of the most common protein modules encoded by metazoan genomes, and is found in many immune system proteins and cell-adhesion molecules (CAMs) [29]. It is composed of a two-sheet sandwich of anti-parallel β strands which adopt a Greek key topology encasing a disulfide bond-stabilized hydrophobic core. The number and location of the β strands can vary between Ig domains. Loop regions between the β strands often exhibit local disorder when examined in the context of the protein crystal, indicating inherent flexibility [30]. All of these structural features are present in the $\beta 3$ Ig domain, including a buried disulfide bond Cys21–96 connecting the two faces. However, to promote trimerization, the $\beta 3$ Ig domain also has a more

unusual region of secondary structure. In most Ig domains, the amino-terminal amino acids are held in place by an anti-parallel β strand [30]. This feature is absent in $\beta 3$. Instead, the region is stabilized by a surface disulfide bond (Cys2–24) and a salt bridge between residues Glu4 and Arg115. Consequently, the hydrophobic amino acids Val3, Val5 and Pro6 are forced into a surface-exposed conformation that forms the core of the trimer interface (figure 3b). Replacing residue Cys24 with alanine in a C24A mutant prevents the formation of the Cys2–24 disulfide bond and reduces trimer stability, presumably because it interferes with the correct alignment of the trimer interface [27].

The α -helical transmembrane domain of the $\beta 3$ subunit contains a conserved glutamic acid residue [23]. Peptides encoding transmembrane α -helices with a membrane-embedded glutamic acid readily form dimers and trimers,

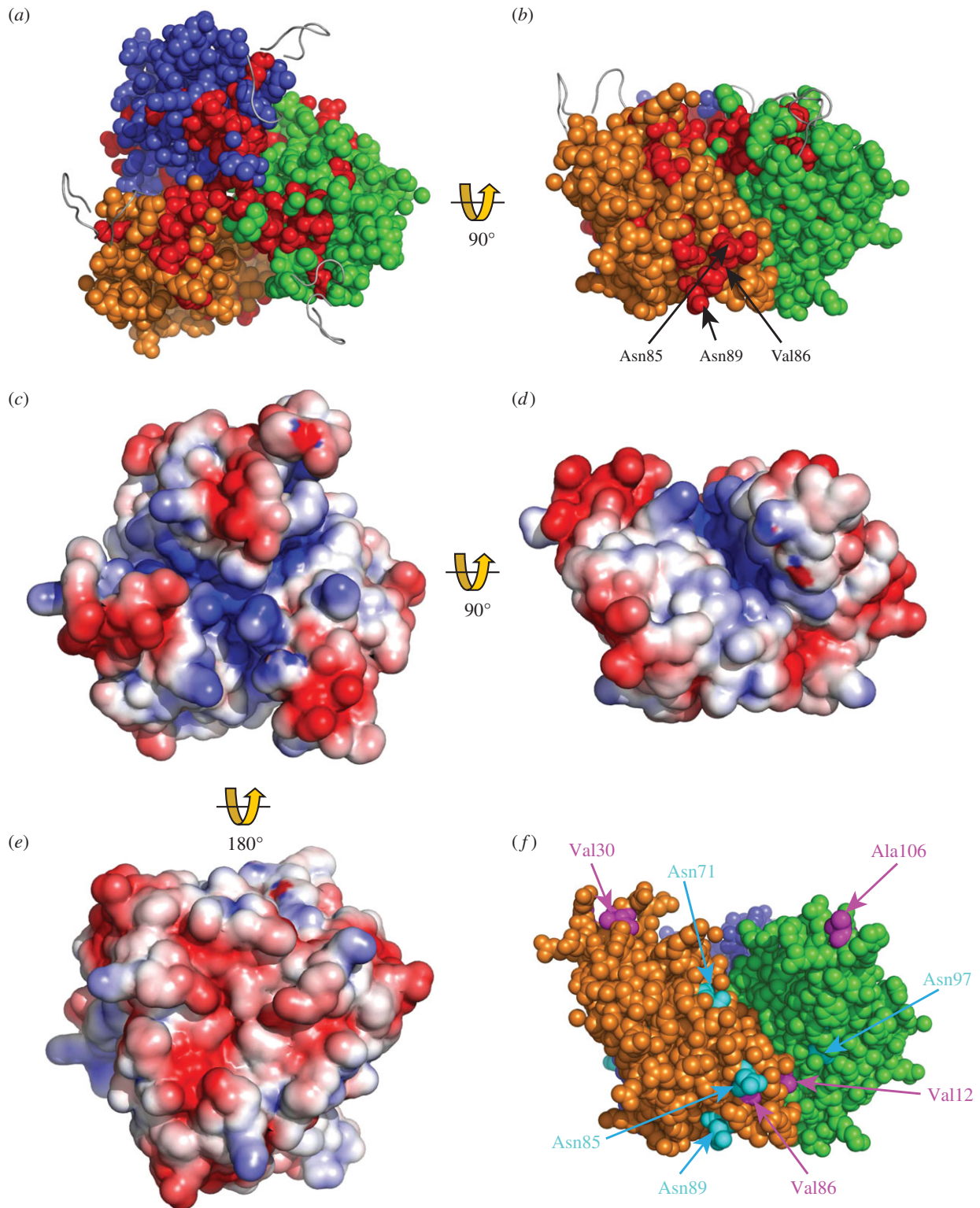


Figure 4. Structural features of the β_3 trimer. (a,b) Evolutionary trace analysis [25] showing residues in red that are identical between β_3 and β_1 in all species for which sequences are available, and mapped onto the β_3 trimer in (a) top and (b) side view. The location of putative N-linked glycosylation sites Asn85 and Asn89, and the cardiopathology mutation V86 within a distinct patch of conserved residues (as mentioned in the text), are indicated for the orange protomer. Disordered loops are shown as grey ribbon. (c–e) Electrostatic surface potential (ESP) of β_3 trimers in (c) top, (d) side and (e) bottom view. ESP was calculated for the trimer surface using the Adaptive Poisson-Boltzmann Solver (APBS) plug-in tool in PyMol [33]. (f) The side face of the trimer showing the location of N-linked glycosylation sites (cyan) and the location of separate cardiopathology mutations (purple) mentioned in the text.

stabilized by hydrogen bonds between the protonated glutamic acid side chains [31]. We have therefore suggested that the transmembrane glutamic acid residue acts to further stabilize a full-length β_3 trimer [27]. A cartoon of the proposed structure for the full-length β_3 trimer is shown in figure 3c.

Residues between β_3 and β_1 that are identical in all species can be identified using evolutionary trace analysis

[32]. In figure 4a,b, these amino acids are mapped onto the trimeric β_3 Ig domain structure. Most of the trimer interface, including the Cys2 and Cys24 residues, is fully conserved between β_3 and β_1 [25], as are the surrounding amino acids that help to align and stabilize the trimer interface. This includes an unusual inward-pointing arginine residue (Arg100), whose mutation in β_1 is associated with febrile

epilepsy [27,34,35]. The $\beta 3$ Ig domain can interact with $\beta 1$ when the two are co-expressed in the same cell [25], suggesting that the trimer interface is functionally conserved between $\beta 3$ and $\beta 1$. Furthermore, the α -helical transmembrane domain of $\beta 1$ includes the unusual membrane-buried glutamic acid residue noted above, and it occurs in the same location on the transmembrane domain as with $\beta 3$ [23,27]. Hence, many of the key features implicated in $\beta 3$ trimer stability are present in $\beta 1$. All these factors taken together suggest that the $\beta 1$ subunit may also assemble into a trimer in a manner broadly similar to $\beta 3$.

4. Insights into Na_v channel assembly and α subunit gating from the $\beta 3$ Ig domain structure

A trimeric $\beta 3$ structure implies that it may promote the oligomerization of up to three α subunits. Consistent with this, AFM imaging detected heterogeneous complexes containing the cardiac-specific α subunit $\text{Na}_v 1.5$ cross-linked by $\beta 3$ dimers and trimers. The frequency of these α subunit oligomers was reduced to the background level when the $\text{Na}_v 1.5$ α subunit was co-expressed with the trimer-disrupting C24A $\beta 3$ subunit mutant described above [27]. The C24A $\beta 3$ mutant also attenuated the normal $\beta 3$ -induced gating shift in the voltage sensitivity of inactivation for $\text{Na}_v 1.5$ α subunits [20]. Hence the oligomeric status of $\text{Na}_v 1.5$ controlled by $\beta 3$ can affect the electrophysiological properties of the channel.

The $\beta 3$ subunit is expressed in the heart [36], and it plays an important role in cardiac physiology, because the major pathology associated with the *Scn3b*^{-/-} mouse is spontaneous cardiac arrhythmia [37,38]. The *Scn1b*^{-/-} mouse also displays cardiac conduction abnormalities [39]. Evidence that the $\beta 1$ subunit, like its homologue $\beta 3$, can cross-link $\text{Na}_v 1.5$ α subunits is provided by an interesting study by Mercier *et al.* [40]. Here an $\text{Na}_v 1.5$ α subunit mutant associated with the cardiac conduction disease Brugada syndrome (BrS) was retained in the endoplasmic reticulum of cardiomyocytes, leading to reduced peak current. The mutation was also associated with reduced surface expression of the wild-type α subunit, but only if mutant and wild-type α subunits were co-expressed together with $\beta 1$. Other 1.5 α subunit mutations linked to BrS show similar dominant negative behaviour when co-expressed with the wild-type α subunit in cardiomyocytes [41–44]. Dominant negative phenotypes can often be explained in molecular terms when mutant and wild-type subunits are jointly assembled into a multi-subunit complex, but then every complex that contains any mutant subunit is functionally inhibited. As a result, heterozygous individuals expressing one mutant and one wild-type copy of a protein display a much greater than 50% reduction of the functional protein activity [45]. We suggest that, *in vivo*, individual $\text{Na}_v 1.5$ α subunits do not behave as independent molecules, but as oligomeric complexes in which multiple α subunits co-assemble, and which the $\beta 3$ and $\beta 1$ subunits may help stabilize. This may help explain why inherited Na_v channel cardiopathologies often behave as autosomal dominant phenotypes in pedigree analysis studies [46].

In many—although by no means all—cell-expression systems, the $\beta 3$ and $\beta 1$ subunits shift the half maximal voltage $V_{1/2}$ for channel activation and inactivation by up to 15 mV

in the hyperpolarizing direction (i.e. the voltages corresponding to activation or inactivation of half the channels are displaced to more negative values compared to corresponding values shown by the α subunit alone; the action potential threshold therefore assumes a more negative voltage, leading to an increased likelihood of firing; figure 1). With α subunit partners such as $\text{Na}_v 1.2$, 1.3 and 1.5, Ig domains of $\beta 3$ and $\beta 1$ are largely responsible for these gating shifts [20,21,23,24,47]. To understand how they might influence gating, we need to consider the structure and location of the β subunit binding site(s) on the α subunits. Unfortunately, the detailed answer to this question is uncertain; even the $\alpha : \beta$ stoichiometry is not clear. Although the conventional view assumes that individual β subunits bind α subunits at a single site [16], there is no over-riding reason to think that this is correct in all cases. In fact, AFM images show that $\beta 3$ can bind to $\text{Na}_v 1.5$ α subunits at up to four locations around the α subunit [27], probably corresponding to sites on each of the four α subunit domains. On the other hand, the pseudo-symmetry of the vertebrate α subunit domains means that there is no requirement for each binding site to be thermodynamically or structurally equivalent. These experiments were also conducted with a high level of $\beta 3$ expression, and without the presence of other β subunits, so not all of the potential sites may be occupied by $\beta 3$ in neurons or myocytes. Nevertheless, they establish the fact that at least under some conditions, a given type of β subunit can bind to the α subunit at multiple locations.

There is currently no molecular information concerning the $\beta 3$ Ig domain binding site(s) on the α subunit. However, given the structural similarity between the $\beta 1$ and $\beta 3$ subunit Ig domains (figure 4*a,b*), it is at least plausible that these two closely related β subunits may bind similar or overlapping sites. The intracellular regions of both $\beta 1$ and $\beta 3$ do indeed bind to similar sites on the $\text{Na}_v 1.5$ α subunit carboxy-terminus [48]. This would indicate that both $\beta 1$ and $\beta 3$ can interact with the α subunit close to domain IV (figure 2*a*). Interestingly, the local anaesthetic lignocaine binds to the S6 helix of domain IV [49], and both $\beta 3$ and $\beta 1$ attenuate lignocaine binding to $\text{Na}_v 1.3$ [50]. A binding site for the $\beta 1$ Ig domain has been localized to the domain IV extracellular S5–S6 region of the brain-type α subunit $\text{Na}_v 1.2$ [51]. In a separate study, two $\beta 1$ -binding sites on the muscle $\text{Na}_v 1.4$ α subunit were mapped to the extracellular regions connecting the S5–S6 helices of domain I and domain IV (figure 2*a*) [52]. If the bacterial Na_v channel structures accurately reflect the topology of the vertebrate Na_v channel, then these two $\beta 1$ binding sites probably lie about 30–40 Å from each other (figure 2*b*). Since the three-dimensional structure of these α subunit extracellular regions is currently unknown, it is not yet possible to say whether they extend far enough to form a joint binding site. Assuming a top-view clockwise arrangement of the α subunit domains [3], the S5–S6 extracellular region of domain I lies closest to the voltage sensor of domain IV, while the S5–S6 extracellular region of domain IV abuts the voltage sensor of domain III. If $\beta 1$ is like $\beta 3$ and forms a trimer, then viewed from above, its shape will be an approximate equilateral triangle of side length about 60 Å (figure 3*c*). Based on the dimensions of the bacterial channel, adjacent voltage sensors will be about 60–70 Å apart. Hence, the Ig domains of $\beta 1$ (and $\beta 3$) at this site could lie close to the α subunit voltage sensors of both domains IV and III. How then could they influence voltage gating sensitivity?

A hyperpolarizing shift could occur if a negatively charged protein is brought sufficiently close to a voltage sensor so that it generates screening surface charge [53–56]. The calculated isoelectric points of the $\beta 1$ and the $\beta 3$ Ig domains are 4.95 and 5.28, respectively, so they will both carry a net negative charge at pH 7.4. Interestingly, the electrostatic surface potential of the $\beta 3$ trimer suggests a dipole-like quality. Positive charges are concentrated on the top surface and the clefts between protomers, although the loop regions at each trimer vertex are negatively charged (figure 4c,d). By contrast, the trimer underside presents negative charges concentrated within a centrally located, shallowly concave face (figure 4e). The full significance of this curious feature will remain unclear until the atomic resolution structure(s) of the $\beta 3$ -binding sites on the α subunit are determined. But it is consistent with a role in presenting negative charge to the α subunit voltage sensors.

An important consideration is that, *in vivo*, the β subunit Ig domains are heterogeneously glycosylated [25,57]. Asparagine (N)-linked glycosylation sites are defined by a conserved Asn-X-(Ser/Thr) motif, in which X can be any amino acid except proline [58] and mature N-linked sugar residues often contain sialic acid moieties on their terminal branches [59]. When tested in CHO cells with Na_v 1.2, 1.5 and 1.7, the hyperpolarizing gating shifts induced by $\beta 1$ were abolished, both by mutagenic removal of the N-linked sites and by using a cell-line lacking sialyl transferase [60]. This indicates an important role for sialylation of the $\beta 1$ Ig domain N-linked glycosylation sites in modulating the gating voltage shifts. The same post-translational modifications will undoubtedly occur on the $\beta 3$ Ig domain. There are four potential N-linked glycosylation sites per $\beta 3$ Ig domain protomer, and all of them point outwards from the surface-exposed faces of the trimer [27] (figure 4f). The potential N-linked glycosylation sites Asn85 and Asn89 are particularly interesting. They are fully conserved between $\beta 3$ and $\beta 1$ in all known species (figure 4b), as are the immediately surrounding residues Val86, Thr87 and Gly92 [25,27]. Furthermore, these two N-linked glycosylation sites lie close to two amino acids that are separately mutated in different inherited cardiopathologies: V86I [61] and V12M [62] (figure 4f). Residue V12 normally forms a hydrophobic contact with Leu116 of an adjacent protomer that helps maintain the correct trimer organization [27]. The V12M mutation probably destabilizes this interaction. Two further mutations in the $\beta 3$ Ig domain that are associated with inherited cardiopathologies have been described. These are A106V [63] and V30G [64], and occur on adjacent Ig domain loops (figure 4f). In the crystal structure, the conformation of these two regions is unresolved due to local disorder (figure 3a,b) [27]. In other Ig domains, the equivalent loop regions can act as binding sites for interacting proteins. For example, these regions of antibody Fab fragment Ig domains constitute the antigen-binding site [30]. In $\beta 3$, their flexible nature, outwardly pointing locations and associations with cardiopathologies make them plausible candidates for an α subunit binding site—perhaps interacting with the S5–S6 extracellular regions of domains I and IV (and see also §5).

We suggest that the hyperpolarizing shifts in voltage gating shown by the $\beta 3$ and $\beta 1$ subunits are caused by an electrostatic mechanism in which the Ig domain is held in place via binding to extracellular regions of the α subunit. This would position the Ig domains so as to present negative charges from sialic acid residues (and perhaps the proteins

themselves), close enough to one or more voltage sensors to affect gating behaviour, as previously proposed [55,56,60]. It should be noted, however, that in some other expression systems the same β subunits can produce *depolarizing* shifts in the $V_{1/2}$ values for activation and inactivation [65–67]. Furthermore, the magnitude of the shifts can vary between α subunit partners. For example, it has been reported that $\beta 3$ subunits have little or no effects on the gating voltage sensitivity of Na_v 1.8 and Na_v 1.6 [22,68]. It is hard to see how such differences can arise, other than by variations in post-translational modification and/or cell-specific and isoform-specific differences in the precise molecular organization of the subunits within the channel complex. An additional factor may be the wider molecular environment of the channel. The Na_v channels do not exist in isolation on the plasma membrane, but as part of local protein clusters that include other ion channels and CAMs [69]. The influence of this clustering on β subunit-induced gating shifts remains to be characterized.

The $\beta 3$ and $\beta 1$ subunits can also enhance the rate of inactivation and recovery from inactivation, and increase the fraction of channels that gate in a fast-acting mode [23,70,71]. Within the α subunit, the carboxy-terminal domain binds to the inactivation gate, and this interaction stabilizes fast inactivation [72]. The α subunit carboxy-terminal domain also binds to the intracellular region of $\beta 3$ and $\beta 1$. An epilepsy-associated mutation in the carboxy-terminal domain of Na_v 1.1 disrupts this interaction and attenuates the normal $\beta 1$ -induced enhancement of inactivation [48]. This suggests that these β subunits may facilitate fast inactivation by binding to, and optimally aligning the complex between, the α subunit carboxy-terminal domain and the inactivation gate. NMR studies on the intracellular region $\beta 3$ intracellular region indicate that it is largely disordered, but with a short juxtamembrane sequence that can adopt a negatively charged amphipathic α -helix [65] (figure 3c). The intracellular regions are long enough to form a complex with the α subunit carboxy-terminus and the inactivation gate. But the formation of α subunit oligomers via $\beta 3$ - and $\beta 1$ -induced cross-linking could greatly facilitate and stabilize these interactions. The Na_v channel oligomer would then behave as an integrated allosteric protein [73]. Consistent with this proposal, it has been shown that mutational disruption of the $\beta 1$ region equivalent to the $\beta 3$ trimer interface reduced the fraction of Na_v 1.2 that acted in the fast-gating mode [74].

5. The $\beta 4$ Ig domain structure and functional implications

The structure of the human $\beta 4$ Ig domain has been solved at 1.7 Å resolution [26]. Overall, the Ig domains of $\beta 4$ and a $\beta 3$ protomer are remarkably similar, despite their low level of sequence similarity (figure 5a,b). However, there are also some striking differences. The most obvious is that the $\beta 4$ Ig domain is a monomer in the crystal asymmetric unit. There is currently no evidence that $\beta 4$ forms *cis* homodimers or homotrimers *in vivo*. Unusually for an Ig domain, the first seven amino-terminal residues (which in $\beta 3$ comprise the trimer interface) are disordered and unresolved in the $\beta 4$ Ig domain crystal structure. There are also significant sequence differences in this region between $\beta 4$ and $\beta 3$. In particular, the C2–24 disulfide bond is not present in $\beta 4$, because the equivalent cysteine residue at position 2 is not present. The Cys24-equivalent residue is present in $\beta 4$ as

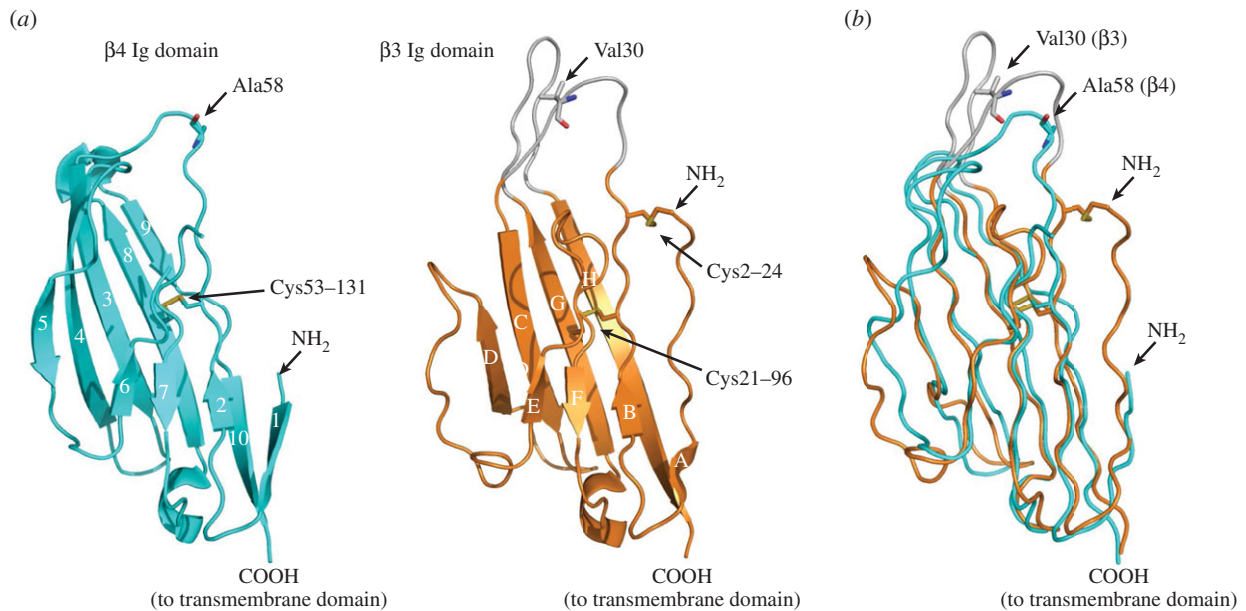


Figure 5. The atomic resolution structure of the $\beta 4$ subunit Ig domain. (a) The $\beta 4$ Ig domain (PDB ID code 4MZZ) and comparison with similar orientation with the $\beta 3$ Ig domain. (b) Supposition of the $\beta 4$ Ig domain (cyan) and a single $\beta 3$ Ig domain protomer (orange), showing the location of the Ala58 residue (corresponding to the free Cys58 residue of $\beta 4$) and the Val30 residue of $\beta 3$ mentioned in the text.

Cys58, but to avoid potential complications caused by the presence of a free cysteine, this residue was mutated to alanine in the protein used for crystallization. The Cys58 residue forms a disulfide bond with the α subunit *in vivo* [18], and so must be located within an α subunit binding site of the $\beta 4$ subunit. Residue 58 is surrounded by side chains of bulky hydrophobic amino acids—particularly Phe59, which is exposed and outward-pointing in the crystal [26], but which is probably buried into a suitable hydrophobic pocket on the α subunit when correctly assembled *in vivo*. Interestingly, residue 58 is located on one of the $\beta 4$ Ig domain surface loops, although the region appears notably less flexible than the corresponding loop in the $\beta 3$ protomer (figure 5a) [26]. When the $\beta 4$ and $\beta 3$ structures are overlaid (figure 5b), the region of $\beta 4$ surrounding residue 58 directly corresponds to the loop region of $\beta 3$ that contains the V30G cardiopathology mutation noted above (figure 4f). This provides some additional evidence that the loop regions of the β subunit Ig domains may be α subunit binding sites (see §4).

In common with most Ig domains, the $\beta 4$ structure contains a buried disulfide bond (C53–131) (figure 5a) [30]. The conventional view has been that the disulfide bond stabilizes Ig domain folding by covalently connecting the two β sheet faces. Surprisingly, however, a C131W mutation still folded and was efficiently exported to the plasma membrane through the secretory pathway. Rather than completely disrupting folding, X-ray crystallographic analysis revealed that the C131W mutation had a more subtle and interesting effect. Breaking the internal disulfide bond led to a local remodelling of the β sheets surrounding the Cys58-containing loop region [26]. This work has important implications for other β subunits. In particular, an equivalent mutation (C121W) in $\beta 1$ causes generalized epilepsy with febrile seizures plus (GEFS+). Here, the mutant $\beta 1$ subunit can no longer bind to and modulate the brain-specific Na_v 1.2 α subunit [75]. It is therefore probable that in $\beta 1$, the C121W mutation selectively perturbs an α subunit interaction site on the $\beta 1$ Ig domain loop region.

The $\beta 4$ binding site(s) on the α subunit are unclear. However, one clue comes from the ability of $\beta 4$ to inhibit toxin-binding. For example, co-expression of $\beta 4$ with the Na_v 1.2 α subunit reduced the affinity of the tarantula toxin ProTx-II for the channel, and $\beta 4$ also reduced sodium influx in Na_v 1.2 when tested with the scorpion toxin TsVII [26]. The ProTx-II toxin binds to the α subunit voltage sensors of domains I, II and IV, and TsVII binds predominantly to the α subunit voltage sensor of domain II [10]. On this basis, it has been suggested that $\beta 4$ may influence the domain II voltage sensor [26]. This presumed $\beta 4$ binding site on the α subunit is different from the one known $\beta 1$ binding site noted above, and Na_v 1.1 channels can be isolated containing both non-covalently associated $\beta 1$ and covalently bound $\beta 4$ subunits [76]. On the other hand, under conditions of high expression, $\beta 4$ can partially (but not completely) displace $\beta 1$ from Na_v 1.1 [76]. Hence, a more subtle possibility is that the $\beta 4$ and $\beta 1$ subunits may bind at more than one site on this α subunit, some of which are overlapping. This is reminiscent of the multiple $\beta 3$ binding sites on Na_v 1.5 detected by AFM and noted earlier. If so, then there are some interesting implications. In neurons, expression of the α and β subunit isoforms can change significantly, both during development [77] and in some pathologies such as diabetic neuropathy [78] and neuropathic pain [79]. If $\beta 3$ and $\beta 1$ can induce α subunit cross-linking, while monomeric $\beta 4$ cannot, then varying expression of different structural classes of β subunits may differentially modulate the oligomeric state of the channels, and this will contribute to both structural and functional heterogeneity within the Na_v channels on the plasma membrane.

A unique aspect of $\beta 4$ behaviour is its ability to promote ‘resurgent current’. This phenomenon occurs when channels are opened by membrane depolarization but are rapidly blocked by an endogenous protein that inhibits current flow, yet also prevents binding of the fast inactivation gate to the pore. Following membrane repolarization, the blocker is removed, leading to a brief resurgent current flow before the

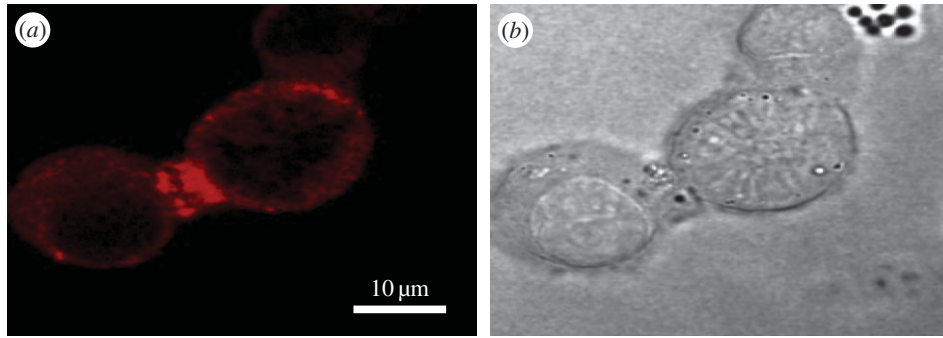


Figure 6. The rat neuronal-like cell-line PC12 expresses the $\beta 3$ subunit endogenously [23]. (a) $\beta 3$ accumulation at the contact site between two PC12 cells, as detected by immunofluorescence microscopy, and (b) DIC image of the same cells. Cells were stained with an affinity-purified rabbit polydonal antibody raised against a $\beta 3$ -specific peptide corresponding to the intracellular region of the molecule. The antibody has been described previously. It detects $\beta 3$ in both Western blotting and immunohistochemistry experiments, and its binding is inhibited by prior incubation with the immunizing peptide [92]. The PC12 cells were fixed, permeabilized and stained as described previously [93].

channels inactivate via the conventional pathway [80]. The blocking factor has been localized to sequences within the $\beta 4$ intracellular region [81]. As with $\beta 3$, the secondary structure of the $\beta 4$ intracellular region is predominantly disordered, but with a short segment adjacent to the membrane that displays amphipathic α -helical potential—although in the case of $\beta 4$, the charges along one face of the helix are positive. It is these charges that are critical for the resurgent current effect [82]. Disordered regions of proteins can sample many different conformations simultaneously, and can provide high-specificity binding even with low intrinsic affinity [83]. They may be advantageous in situations encountered by the intracellular regions of both $\beta 3$ and $\beta 4$, with their requirement for different binding interactions occurring at specific parts in the channel gating cycle.

The $\beta 4$ subunit is closest in sequence identity to $\beta 2$. The $\beta 2$ subunit also contains a free cysteine at the equivalent position to Cys58, and likewise forms a disulfide bond with the α subunit *in vivo* [19]. However, it is not known if $\beta 2$ and $\beta 4$ share overlapping binding sites. For $\text{Na}_v 1.5$, the $\beta 2$ subunit induces hyperpolarizing gating shifts that are sialic-acid-dependent [84]. On the other hand, the $\beta 2$ subunit induces sialic-acid-independent depolarizing gating shifts for $\text{Na}_v 1.2$ [84]. There are currently no structural explanations for these strikingly disparate effects. Again, they emphasize the complex isoform-specific nature of the binding interactions between $\text{Na}_v \alpha$ and β subunits. Mice lacking $\beta 2$ expression have a relatively mild phenotype, although they are more prone to seizures. Interestingly, these mice display a significantly reduced Na_v channel density in some classes of neurons, especially in the hippocampus [85]. It is therefore possible that $\beta 2$ has a particularly important role in stabilizing Na_v channels in the plasma membrane [86].

6. The $\text{Na}_v \beta$ subunits as cell-adhesion molecules

The $\text{Na}_v \beta$ subunits are related to members of the CAMs superfamily [17], and there is growing evidence that β subunits display CAM-like behaviour both in *cis* and in *trans*. The $\beta 1$ subunit Ig domain can interact in *cis* with other CAMs such as neurofascin-155 and neurofascin-186, contactins and cadherins, and $\beta 3$ can bind neurofascin-186

[87,88]. The $\beta 1$ and $\beta 2$ subunits interact with extracellular matrix proteins such as tenascin-R that are secreted by oligodendrocytes during myelination [89]. These multiple interactions all help localize Na_v channels to discrete clusters at the nodes of Ranvier in myelinated neurons, and probably increase the total amount of Na_v channels in the membrane.

The $\text{Na}_v \beta$ subunits also act as *trans*-binding CAMs independently of α subunits. This has been conveniently studied by expressing them in the *Drosophila* S2 cell-line and monitoring cell adhesion visually. Here, the $\beta 1$ and $\beta 2$ subunits promoted cell adhesion [90], while the $\beta 3$ subunit did not [91]. On the other hand, $\beta 3$ -mediated cell adhesion was detected when assayed in more physiologically mammalian cell-lines, both by immunoprecipitation [25] and by immunofluorescence (figure 6). The *trans* cell adhesion of $\beta 3$ -subunits required an intact Cys2–24 disulfide bond [25]. Hence, the *cis*-formed $\beta 3$ trimer is probably needed to form the *trans*-binding cell–cell contacts. This is similar to the behaviour shown by the CAM myelin P0 which stabilizes the myelin sheath around peripheral neurons [94]. The myelin P0 molecules assemble as tetramers in *cis*, and then the tetramers associate in *trans* to form tight intercellular contacts [94]. It may be significant that myelin P0 is a distant paralogue of the $\text{Na}_v \beta$ subunits, and its Ig domain has previously been used to model both the $\beta 1$ and $\beta 3$ Ig domains [23,25,74,95].

The demonstration that at least some β subunits have both *cis* and *trans* CAM activity complicates the interpretation of knockout mouse phenotypes. For example, rapid conduction in the heart requires the cardiomyocytes to be electrically coupled to each other via their apposed intercalated discs [46,96]. The β subunits are located on the intercalated discs of ventricular cardiomyocytes [38,97,98], and their absence will probably have multiple effects: the Na_v channels will display altered gating behaviour and their location at the intercalated discs may be destabilized, but cell adhesion between cardiomyocytes could also be compromised, potentially leading to loss of signal cohesion during the intercellular propagation of the cardiac action potential. We should be open to the possibility that some of the pathologies shown by β subunit knockout mice (and by the human pathologies associated with β subunit mutations) reflect abnormalities in cell adhesion rather than direct electrophysiological effects on the Na_v channels themselves.

7. Summary

An earlier review described Na_v channel β subunits as ‘anything but auxiliary’ [99]. We agree with this sentiment, and we emphasize the integration of the β subunits with other Na_v channel components. As a case in point, we note the current interest in the pharmacological potential of animal toxins that target Na_v channels [100]. In some examples, the binding affinity of these toxins for Na_v channels is actually *increased* by the presence of specific β subunits [101,102]. This raises interesting questions about the nature of the toxin-binding sites. The important point is that these toxins evolved to act against Na_v channels in their normal physiological context, which includes the β subunits. We suggest that screening assays for such toxins

and drugs should include, wherever possible, the relevant β subunit(s) for the Na_v channels in question.

These are interesting times for Na_v channel β subunit research. The new results from X-ray crystallography and molecular imaging provide the first detailed look at the molecules, and will encourage both the generation of detailed functional hypotheses and their experimental testing.

Acknowledgements. We thank Manoj Patel, Bojana Popovic and Trevor Wilkinson for their helpful comments on the manuscript.

Funding statement. S.N. is supported by a Cambridge Nehru Trust scholarship. D.Y.C. is funded by the Crystallographic X-ray Facility, Department of Biochemistry, University of Cambridge. C.L.-H.H. is funded by the Medical Research Council (UK) grant MR/M001288/1 and the MacVeigh Benefaction.

References

- Waxman SG. 2012 Sodium channels, the electrogenosome and the electrogenistat: lessons and questions from the clinic. *J. Physiol.* **590**, 2601–2612. (doi:10.1113/jphysiol.2012.228460)
- Mantegazza M, Catterall WA. 2012 Voltage-gated Na⁺ channels: structure, function, and pathophysiology. In *Jasper's basic mechanisms of the epilepsies* (eds JL Noebels, M Avoli, MA Rogawski, RW Olsen, AV Delgado-Escueta). Bethesda, MD.
- Dudley Jr SC, Chang N, Hall J, Lipkind G, Fozzard HA, French RJ. 2000 μ-conotoxin GIIIA interactions with the voltage-gated Na⁺ channel predict a clockwise arrangement of the domains. *J. Gen. Physiol.* **116**, 679–690. (doi:10.1085/jgp.116.5.679)
- Payandeh J, Scheuer T, Zheng N, Catterall WA. 2011 The crystal structure of a voltage-gated sodium channel. *Nature* **475**, 353–358. (doi:10.1038/nature10238)
- Zhang X *et al.* 2012 Crystal structure of an orthologue of the NaChBac voltage-gated sodium channel. *Nature* **486**, 130–134. (doi:10.1038/nature11054)
- McCusker EC, Bagneris C, Naylor CE, Cole AR, D'Avanzo N, Nichols CG, Wallace BA. 2012 Structure of a bacterial voltage-gated sodium channel pore reveals mechanisms of opening and closing. *Nat. Commun.* **3**, 1102. (doi:10.1038/ncomms2077)
- Long SB, Tao X, Campbell EB, MacKinnon R. 2007 Atomic structure of a voltage-dependent K⁺ channel in a lipid membrane-like environment. *Nature* **450**, 376–382. (doi:10.1038/nature06265)
- Catterall WA. 2012 Voltage-gated sodium channels at 60: structure, function and pathophysiology. *J. Physiol.* **590**, 2577–2589. (doi:10.1113/jphysiol.2011.224204)
- Chanda B, Bezanilla F. 2002 Tracking voltage-dependent conformational changes in skeletal muscle sodium channel during activation. *J. Gen. Physiol.* **120**, 629–645. (doi:10.1085/jgp.20028679)
- Bosmans F, Martin-Eauclaire MF, Swartz KJ. 2008 Deconstructing voltage sensor function and pharmacology in sodium channels. *Nature* **456**, 202–208. (doi:10.1038/nature07473)
- Capes DL, Goldschen-Ohm MP, Arcisio-Miranda M, Bezanilla F, Chanda B. 2013 Domain IV voltage-sensor movement is both sufficient and rate limiting for fast inactivation in sodium channels. *J. Gen. Physiol.* **142**, 101–112. (doi:10.1085/jgp.201310998)
- Vargas E *et al.* 2012 An emerging consensus on voltage-dependent gating from computational modeling and molecular dynamics simulations. *J. Gen. Physiol.* **140**, 587–594. (doi:10.1085/jgp.201210873)
- Brackenbury WJ, Isom LL. 2011 Na⁺ channel β subunits: overachievers of the ion channel family. *Front. Pharmacol.* **2**, 53. (doi:10.3389/fphar.2011.00053)
- Cusdin FS, Clare JJ, Jackson AP. 2008 Trafficking and cellular distribution of voltage-gated sodium channels. *Traffic* **9**, 17–26. (doi:10.1111/j.1600-0854.2007.00673.x)
- Qin N, D'Andrea MR, Lubin ML, Shafae N, Codd EE, Correa AM. 2003 Molecular cloning and functional expression of the human sodium channel β_{1B} subunit, a novel splicing variant of the β₁ subunit. *Eur. J. Biochem.* **270**, 4762–4770. (doi:10.1046/j.1432-1033.2003.03878.x)
- Patino GA, Isom LL. 2010 Electrophysiology and beyond: multiple roles of Na⁺ channel β subunits in development and disease. *Neurosci. Lett.* **486**, 53–59. (doi:10.1016/j.neulet.2010.06.050)
- Chopra SS, Watanabe H, Zhong TP, Roden DM. 2007 Molecular cloning and analysis of zebrafish voltage-gated sodium channel beta subunit genes: implications for the evolution of electrical signaling in vertebrates. *BMC Evol. Biol.* **7**, 113. (doi:10.1186/1471-2148-7-113)
- Buffington SA, Rasband MN. 2013 Na⁺ channel-dependent recruitment of Na_vβ4 to axon initial segments and nodes of Ranvier. *J. Neurosci.* **33**, 6191–6202. (doi:10.1523/JNEUROSCI.4051-12.2013)
- Chen C, Calhoun JD, Zhang Y, Lopez-Santiago L, Zhou N, Davis TH, Salzer JL, Isom LL. 2012 Identification of the cysteine residue responsible for disulfide linkage of Na⁺ channel α and β2 subunits. *J. Biol. Chem.* **287**, 39 061–39 069. (doi:10.1074/jbc.M112.397646)
- Yu EJ, Ko SH, Lenkowski PW, Pance A, Patel MK, Jackson AP. 2005 Distinct domains of the sodium channel β3-subunit modulate channel-gating kinetics and subcellular location. *Biochem. J.* **392**, 519–526. (doi:10.1042/BJ20050518)
- Chen C, Cannon SC. 1995 Modulation of Na⁺ channel inactivation by the β₁ subunit: a deletion analysis. *Pflügers Arch.* **431**, 186–195. (doi:10.1007/BF00410190)
- Chahine M, O'Leary ME. 2011 Regulatory role of voltage-gated Na⁺ channel β subunits in sensory neurons. *Front. Pharmacol.* **2**, 70. (doi:10.3389/fphar.2011.00070)
- Morgan K *et al.* 2000 β 3: an additional auxiliary subunit of the voltage-sensitive sodium channel that modulates channel gating with distinct kinetics. *Proc. Natl Acad. Sci. USA* **97**, 2308–2313. (doi:10.1073/pnas.030362197)
- McCormick KA, Srinivasan J, White K, Scheuer T, Catterall WA. 1999 The extracellular domain of the β1 subunit is both necessary and sufficient for β1-like modulation of sodium channel gating. *J. Biol. Chem.* **274**, 32 638–32 646. (doi:10.1074/jbc.274.46.32638)
- Yerreddi NR, Cusdin FS, Namadurai S, Packman LC, Monie TP, Slavny P, Clare JJ, Powell AJ, Jackson AP. 2013 The immunoglobulin domain of the sodium channel β3 subunit contains a surface-localized disulfide bond that is required for homophilic binding. *Faseb J.* **27**, 568–580. (doi:10.1096/fj.12-209445)
- Gilchrist J, Das S, Van Petegem F, Bosmans F. 2013 Crystallographic insights into sodium-channel modulation by the β4 subunit. *Proc. Natl Acad. Sci. USA* **110**, E5016–E5024. (doi:10.1073/pnas.1314557110)
- Namadurai S, Balasuriya D, Rajappa R, Wiemhofer M, Stott K, Klingauf J, Edwardson JM, Chirgadze DY, Jackson AP. 2014 Crystal structure and molecular imaging of the Na_v channel β3 subunit indicates a trimeric assembly. *J. Biol. Chem.* **289**, 10 797–10 811. (doi:10.1074/jbc.M113.527994)
- Calhoun JD, Isom LL. 2014 The role of non-pore-forming beta subunits in physiology and

- pathophysiology of voltage-gated sodium channels. *Handb. Exp. Pharmacol.* **221**, 51–89. (doi:10.1007/978-3-642-41588-3_4)
29. Barday AN. 1999 Ig-like domains: evolution from simple interaction molecules to sophisticated antigen recognition. *Proc. Natl Acad. Sci. USA* **96**, 14 672–14 674. (doi:10.1073/pnas.96.26.14672)
 30. Bork P, Holm L, Sander C. 1994 The immunoglobulin fold: structural classification, sequence patterns and common core. *J. Mol. Biol.* **242**, 309–320. (doi:10.1006/jmbi.1994.1582)
 31. Gratkowski H, Lear JD, DeGrado WF. 2001 Polar side chains drive the association of model transmembrane peptides. *Proc. Natl Acad. Sci. USA* **98**, 880–885. (doi:10.1073/pnas.98.3.880)
 32. Lichtarge O, Bourne HR, Cohen FE. 1996 An evolutionary trace method defines binding surfaces common to protein families. *J. Mol. Biol.* **257**, 342–358. (doi:10.1006/jmbi.1996.0167)
 33. Baker NA, Sept D, Joseph S, Holst MJ, McCammon JA. 2001 Electrostatics of nanosystems: application to microtubules and the ribosome. *Proc. Natl Acad. Sci. USA* **98**, 10 037–10 041. (doi:10.1073/pnas.181342398)
 34. Fendri-Kriaa N, Kammoun F, Salem IH, Kifagi C, Mkaouar-Rebai E, Hsairi I, Rebai A, Triki C, Fakhfakh F. 2011 New mutation c.374C > T and a putative disease-associated haplotype within *SCN1B* gene in Tunisian families with febrile seizures. *Eur. J. Neurol.* **18**, 695–702. (doi:10.1111/j.1468-1331.2010.03216.x)
 35. Patino GA *et al.* 2009 A functional null mutation of *SCN1B* in a patient with Dravet syndrome. *J. Neurosci.* **29**, 10 764–10 778. (doi:10.1523/JNEUROSCI.2475-09.2009)
 36. Fahmi Al *et al.* 2001 The sodium channel beta-subunit *SCN3b* modulates the kinetics of *SCN5a* and is expressed heterogeneously in sheep heart. *J. Physiol.* **537**, 693–700. (doi:10.1113/jphysiol.2001.012691)
 37. Hakim P, Gurung IS, Pedersen TH, Thresher R, Brice N, Lawrence J, Grace AA, Huang CL. 2008 *Scn3b* knockout mice exhibit abnormal ventricular electrophysiological properties. *Prog. Biophys. Mol. Biol.* **98**, 251–266. (doi:10.1016/j.pbiomolbio.2009.01.005)
 38. Hakim P, Brice N, Thresher R, Lawrence J, Zhang Y, Jackson AP, Grace AA, Huang CL. 2010 *Scn3b* knockout mice exhibit abnormal sino-atrial and cardiac conduction properties. *Acta Physiol.* **198**, 47–59. (doi:10.1111/j.1748-1716.2009.02048.x)
 39. Lopez-Santiago LF *et al.* 2007 Sodium channel *Scn1b* null mice exhibit prolonged QT and RR intervals. *J. Mol. Cell. Cardiol.* **43**, 636–647. (doi:10.1016/j.yjmcc.2007.07.062)
 40. Mercier A, Clement R, Harnois T, Bourmeyster N, Faivre JF, Findlay I, Chahine M, Bois P, Chatelier A. 2012 The β_1 -subunit of $\text{Na}_v1.5$ cardiac sodium channel is required for a dominant negative effect through α - α interaction. *PLoS ONE* **7**, e48690. (doi:10.1371/journal.pone.0048690)
 41. Hoshi M, Du XX, Shinlapawattayatorn K, Liu H, Chai S, Wan X, Ficker E, Deschenes I. 2014 Brugada syndrome disease phenotype explained in apparently benign sodium channel mutations. *Circ. Cardiovasc. Genet.* **7**, 123–131. (doi:10.1161/CIRCGENETICS.113.000292)
 42. Poelzing S *et al.* 2006 *SCN5A* polymorphism restores trafficking of a Brugada syndrome mutation on a separate gene. *Circulation* **114**, 368–376. (doi:10.1161/CIRCULATIONAHA.105.601294)
 43. Keller DI *et al.* 2005 Brugada syndrome and fever: genetic and molecular characterization of patients carrying *SCN5A* mutations. *Cardiovasc. Res.* **67**, 510–519. (doi:10.1016/j.cardiores.2005.03.024)
 44. Clatot J *et al.* 2012 Dominant-negative effect of *SCN5A* N-terminal mutations through the interaction of $\text{Na}_v1.5$ α -subunits. *Cardiovasc. Res.* **96**, 53–63. (doi:10.1093/cvr/cvs211)
 45. Veitia RA. 2007 Exploring the molecular etiology of dominant-negative mutations. *Plant Cell* **19**, 3843–3851. (doi:10.1105/tpc.107.055053)
 46. Lei M, Huang CL, Zhang Y. 2008 Genetic Na^+ channelopathies and sinus node dysfunction. *Progr. Biophys. Mol. Biol.* **98**, 171–178. (doi:10.1016/j.pbiomolbio.2008.10.003)
 47. Meadows LS, Chen YH, Powell AJ, Clare JJ, Ragsdale DS. 2002 Functional modulation of human brain $\text{Na}_v1.3$ sodium channels, expressed in mammalian cells, by auxiliary β_1 , β_2 and β_3 subunits. *Neuroscience* **114**, 745–753. (doi:10.1016/S0306-4522(02)00242-7)
 48. Spanpanato J *et al.* 2004 A novel epilepsy mutation in the sodium channel *SCN1A* identifies a cytoplasmic domain for beta subunit interaction. *J. Neurosci.* **24**, 10 022–10 034. (doi:10.1523/JNEUROSCI.2034-04.2004)
 49. Ragsdale DS, McPhee JC, Scheuer T, Catterall WA. 1994 Molecular determinants of state-dependent block of Na^+ channels by local anesthetics. *Science* **265**, 1724–1728. (doi:10.1126/science.8085162)
 50. Lenkowski PW, Shah BS, Dinn AE, Lee K, Patel MK. 2003 Lidocaine block of neonatal $\text{Na}_v1.3$ is differentially modulated by co-expression of β_1 and β_3 subunits. *Eur. J. Pharmacol.* **467**, 23–30. (doi:10.1016/S0014-2999(03)01595-4)
 51. Qu Y, Rogers JC, Chen SF, McCormick KA, Scheuer T, Catterall WA. 1999 Functional roles of the extracellular segments of the sodium channel alpha subunit in voltage-dependent gating and modulation by β_1 subunits. *J. Biol. Chem.* **274**, 32 647–32 654. (doi:10.1074/jbc.274.46.32647)
 52. Makita N, Bennett PB, George Jr AL. 1996 Molecular determinants of beta 1 subunit-induced gating modulation in voltage-dependent Na^+ channels. *J. Neurosci.* **16**, 7117–7127.
 53. Mehta AR, Huang CL, Skepper JN, Fraser JA. 2008 Extracellular charge adsorption influences intracellular electrochemical homeostasis in amphibian skeletal muscle. *Biophys. J.* **94**, 4549–4560. (doi:10.1529/biophysj.107.128587)
 54. Chandler WK, Hodgkin AL, Meves H. 1965 The effect of changing the internal solution on sodium inactivation and related phenomena in giant axons. *J. Physiol.* **180**, 821–836.
 55. Ferrera L, Moran O. 2006 Beta1-subunit modulates the $\text{Na}_v1.4$ sodium channel by changing the surface charge. *Exp. Brain Res.* **172**, 139–150. (doi:10.1007/s00221-005-0323-4)
 56. Ednie AR, Bennett ES. 2012 Modulation of voltage-gated ion channels by sialylation. *Compr. Physiol.* **2**, 1269–1301. (doi:10.1002/cphy.c110044)
 57. Isom LL, De Jongh KS, Patton DE, Reber BF, Offord J, Charbonneau H, Walsh K, Goldin AL, Catterall WA. 1992 Primary structure and functional expression of the β_1 subunit of the rat brain sodium channel. *Science* **256**, 839–842. (doi:10.1126/science.1375395)
 58. Bause E. 1983 Structural requirements of N-glycosylation of proteins: studies with proline peptides as conformational probes. *Biochem. J.* **209**, 331–336.
 59. Hart GW. 1992 Glycosylation. *Curr. Opin. Cell Biol.* **4**, 1017–1023. (doi:10.1016/0955-0674(92)90134-X)
 60. Johnson D, Montpetit ML, Stocker PJ, Bennett ES. 2004 The sialic acid component of the β_1 subunit modulates voltage-gated sodium channel function. *J. Biol. Chem.* **279**, 44 303–44 310. (doi:10.1074/jbc.M408900200)
 61. Ishikawa T *et al.* 2013 Novel *SCN3B* mutation associated with brugada syndrome affects intracellular trafficking and function of $\text{Na}_v1.5$. *Circ. J.* **77**, 959–967. (doi:10.1253/circj.CJ-12-0995)
 62. Tan BH, Pundi KN, Van Norstrand DW, Valdivia CR, Tester DJ, Medeiros-Domingo A, Makielski JC, Ackerman MJ. 2010 Sudden infant death syndrome-associated mutations in the sodium channel β subunits. *Heart Rhythm* **7**, 771–778. (doi:10.1016/j.hrthm.2010.01.032)
 63. Wang P *et al.* 2010 Functional dominant-negative mutation of sodium channel subunit gene *SCN3B* associated with atrial fibrillation in a Chinese GenelD population. *Biochem. Biophys. Res. Commun.* **398**, 98–104. (doi:10.1016/j.bbrc.2010.06.042)
 64. Valdivia CR, Medeiros-Domingo A, Ye B, Shen WK, Algiers TJ, Ackerman MJ, Makielski JC. 2010 Loss-of-function mutation of the *SCN3B*-encoded sodium channel β_3 subunit associated with a case of idiopathic ventricular fibrillation. *Cardiovasc. Res.* **86**, 392–400. (doi:10.1093/cvr/cvp417)
 65. Cusdin FS, Nietlispach D, Maman J, Dale TJ, Powell AJ, Clare JJ, Jackson AP. 2010 The sodium channel β_3 -subunit induces multiphasic gating in $\text{Na}_v1.3$ and affects fast inactivation via distinct intracellular regions. *J. Biol. Chem.* **285**, 33 404–33 412. (doi:10.1074/jbc.M110.114058)
 66. Qu Y, Curtis R, Lawson D, Gilbride K, Ge P, DiStefano PS, Silos-Santiago I, Catterall WA, Scheuer T. 2001 Differential modulation of sodium channel gating and persistent sodium currents by the β_1 , β_2 , and β_3 subunits. *Mol. Cell. Neurosci.* **18**, 570–580. (doi:10.1006/mcne.2001.1039)
 67. Cummins TR, Aglioco F, Renganathan M, Herzog RI, Dib-Hajj SD, Waxman SG. 2001 $\text{Nav}1.3$ sodium channels: rapid repriming and slow closed-state inactivation display quantitative differences after expression in a mammalian cell line and in spinal sensory neurons. *J. Neurosci.* **21**, 5952–5961.

68. Zhao J, O'Leary ME, Chahine M. 2011 Regulation of Nav1.6 and Nav1.8 peripheral nerve Na⁺ channels by auxiliary β -subunits. *J. Neurophysiol.* **106**, 608–619. (doi:10.1152/jn.00107.2011)
69. Letterier C, Brachet A, Dargent B, Vacher H. 2011 Determinants of voltage-gated sodium channel clustering in neurons. *Semin. Cell Dev. Biol.* **22**, 171–177. (doi:10.1016/j.semdb.2010.09.014)
70. Patton DE, Isom LL, Catterall WA, Goldin AL. 1994 The adult rat brain β 1 subunit modifies activation and inactivation gating of multiple sodium channel alpha subunits. *J. Biol. Chem.* **269**, 17 649–17 655.
71. Bennett Jr PB, Makita N, George Jr AL. 1993 A molecular basis for gating mode transitions in human skeletal muscle Na⁺ channels. *FEBS Lett.* **326**, 21–24. (doi:10.1016/0014-5793(93)81752-L)
72. Motoike HK, Liu H, Glaaser IW, Yang AS, Tateyama M, Kass RS. 2004 The Na⁺ channel inactivation gate is a molecular complex: a novel role of the COOH-terminal domain. *J. Gen. Physiol.* **123**, 155–165. (doi:10.1085/jgp.200308929)
73. Changeux JP. 2012 Allosteric and the Monod–Wyman–Changeux model after 50 years. *Annu. Rev. Biophys.* **41**, 103–133. (doi:10.1146/annurev-biophys-050511-102222)
74. McCormick KA, Isom LL, Ragsdale D, Smith D, Scheuer T, Catterall WA. 1998 Molecular determinants of Na⁺ channel function in the extracellular domain of the beta1 subunit. *J. Biol. Chem.* **273**, 3954–3962. (doi:10.1074/jbc.273.7.3954)
75. Wallace RH *et al.* 1998 Febrile seizures and generalized epilepsy associated with a mutation in the Na⁺-channel β 1 subunit gene SCN1B. *Nat. Genet.* **19**, 366–370. (doi:10.1038/1252)
76. Aman TK, Grieco-Calub TM, Chen C, Rusconi R, Slat EA, Isom LL, Raman IM. 2009 Regulation of persistent Na current by interactions between beta subunits of voltage-gated Na channels. *J. Neurosci.* **29**, 2027–2042. (doi:10.1523/JNEUROSCI.4531-08.2009)
77. Shah BS, Gonzalez MI, Bramwell S, Pinnock RD, Lee K, Dixon AK. 2001 β 3, a novel auxiliary subunit for the voltage gated sodium channel is upregulated in sensory neurones following streptozocin induced diabetic neuropathy in rat. *Neurosci. Lett.* **309**, 1–4. (doi:10.1016/S0304-3940(01)01976-0)
78. Craner MJ, Klein JP, Renganathan M, Black JA, Waxman SG. 2002 Changes of sodium channel expression in experimental painful diabetic neuropathy. *Ann. Neurol.* **52**, 786–792. (doi:10.1002/ana.10364)
79. Shah BS, Stevens EB, Gonzalez MI, Bramwell S, Pinnock RD, Lee K, Dixon AK. 2000 β 3, a novel auxiliary subunit for the voltage-gated sodium channel, is expressed preferentially in sensory neurons and is upregulated in the chronic constriction injury model of neuropathic pain. *Eur. J. Neurosci.* **12**, 3985–3990. (doi:10.1046/j.1460-9568.2000.00294.x)
80. Bean BP. 2005 The molecular machinery of resurgent sodium current revealed. *Neuron* **45**, 185–187. (doi:10.1016/j.neuron.2005.01.006)
81. Grieco TM, Malhotra JD, Chen C, Isom LL, Raman IM. 2005 Open-channel block by the cytoplasmic tail of sodium channel beta4 as a mechanism for resurgent sodium current. *Neuron* **45**, 233–244. (doi:10.1016/j.neuron.2004.12.035)
82. Lewis AH, Raman IM. 2011 Cross-species conservation of open-channel block by Na channel beta4 peptides reveals structural features required for resurgent Na current. *J. Neurosci.* **31**, 11 527–11 536. (doi:10.1523/JNEUROSCI.1428-11.2011)
83. Liu Z, Huang Y. 2014 Advantages of proteins being disordered. *Protein Sci.* **23**, 539–550. (doi:10.1002/pro.2443)
84. Johnson D, Bennett ES. 2006 Isoform-specific effects of the beta2 subunit on voltage-gated sodium channel gating. *J. Biol. Chem.* **281**, 25 875–25 881. (doi:10.1074/jbc.M605060200)
85. Chen C *et al.* 2002 Reduced sodium channel density, altered voltage dependence of inactivation, and increased susceptibility to seizures in mice lacking sodium channel β 2-subunits. *Proc. Natl Acad. Sci. USA* **99**, 17 072–17 077. (doi:10.1073/pnas.212638099)
86. Schmidt JW, Catterall WA. 1986 Biosynthesis and processing of the alpha subunit of the voltage-sensitive sodium channel in rat brain neurons. *Cell* **46**, 437–444. (doi:10.1016/0092-8674(86)90664-1)
87. Ratcliffe CF, Westenbroek RE, Curtis R, Catterall WA. 2001 Sodium channel β 1 and β 3 subunits associate with neurofascin through their extracellular immunoglobulin-like domain. *J. Cell Biol.* **154**, 427–434. (doi:10.1083/jcb.200102086)
88. Kazarinova-Noyes K *et al.* 2001 Contactin associates with Na⁺ channels and increases their functional expression. *J. Neurosci.* **21**, 7517–7525.
89. Xiao ZC, Ragsdale DS, Malhotra JD, Mattei LN, Braun PE, Schachner M, Isom LL. 1999 Tenascin-R is a functional modulator of sodium channel beta subunits. *J. Biol. Chem.* **274**, 26 511–26 517. (doi:10.1074/jbc.274.37.26511)
90. Malhotra JD, Kazen-Gillespie K, Hortsch M, Isom LL. 2000 Sodium channel beta subunits mediate homophilic cell adhesion and recruit ankyrin to points of cell–cell contact. *J. Biol. Chem.* **275**, 11 383–11 388. (doi:10.1074/jbc.275.15.11383)
91. McEwen DP, Chen C, Meadows LS, Lopez-Santiago L, Isom LL. 2009 The voltage-gated Na⁺ channel beta3 subunit does not mediate trans homophilic cell adhesion or associate with the cell adhesion molecule contactin. *Neurosci. Lett.* **462**, 272–275. (doi:10.1016/j.neulet.2009.07.020)
92. van Gassen KL, de Wit M, van Kempen M, van der Hel WS, van Rijen PC, Jackson AP, Lindhout D, de Graan PN. 2009 Hippocampal Na β 3 expression in patients with temporal lobe epilepsy. *Epilepsia* **50**, 957–962. (doi:10.1111/j.1528-1167.2008.02015.x)
93. Pance A, Morgan K, Guest PC, Bowers K, Dean GE, Cutler DF, Jackson AP. 1999 A PC12 variant lacking regulated secretory organelles: aberrant protein targeting and evidence for a factor inhibiting neuroendocrine gene expression. *J. Neurochem.* **73**, 21–30. (doi:10.1046/j.1471-4159.1999.0730021.x)
94. Spiryda LB. 1998 Myelin protein zero and membrane adhesion. *J. Neurosci. Res.* **54**, 137–146. (doi:10.1002/(SICI)1097-4547(19981015)54:2<137::AID-JNR2>3.0.CO;2-F)
95. Islas AA, Sanchez-Solano A, Scior T, Millan-PerezPenal L, Salinas-Stefanon EM. 2013 Identification of Navbeta1 residues involved in the modulation of the sodium channel Na_v1.4. *PLoS ONE* **8**, e81995. (doi:10.1371/journal.pone.0081995)
96. Meadows LS, Isom LL. 2005 Sodium channels as macromolecular complexes: implications for inherited arrhythmia syndromes. *Cardiovasc. Res.* **67**, 448–458. (doi:10.1016/j.cardiores.2005.04.003)
97. Malhotra JD, Thyagarajan V, Chen C, Isom LL. 2004 Tyrosine-phosphorylated and nonphosphorylated sodium channel β 1 subunits are differentially localized in cardiac myocytes. *J. Biol. Chem.* **279**, 40 748–40 754. (doi:10.1074/jbc.M407243200)
98. Maier SK, Westenbroek RE, McCormick KA, Curtis R, Scheuer T, Catterall WA. 2004 Distinct subcellular localization of different sodium channel alpha and beta subunits in single ventricular myocytes from mouse heart. *Circulation* **109**, 1421–1427. (doi:10.1161/01.CIR.0000121421.61896.24)
99. Isom LL. 2001 Sodium channel beta subunits: anything but auxiliary. *Neuroscientist* **7**, 42–54. (doi:10.1177/107385840100700108)
100. Billen B, Bosmans F, Tytgat J. 2008 Animal peptides targeting voltage-activated sodium channels. *Curr. Pharm. Des.* **14**, 2492–2502. (doi:10.2174/138161208785777423)
101. Zhang MM, Wilson MJ, Azam L, Gajewiak J, Rivier JE, Bulaj G, Olivera BM, Yoshikami D. 2013 Co-expression of Na_vbeta subunits alters the kinetics of inhibition of voltage-gated sodium channels by pore-blocking μ -conotoxins. *Br. J. Pharmacol.* **168**, 1597–1610. (doi:10.1111/bph.12051)
102. Wilson MJ, Zhang MM, Azam L, Olivera BM, Bulaj G, Yoshikami D. 2011 Navbeta subunits modulate the inhibition of Na_v1.8 by the analgesic gating modifier μ 0-conotoxin MrVIB. *J. Pharmacol. Exp. Ther.* **338**, 687–693. (doi:10.1124/jpet.110.178343)